Non-Fullerene Acceptors of IDIC/ITIC Families

Subjects: Polymer Science

Contributor: Dario Pasini

IDIC/ITIC families of non-fullerene acceptors has boosted the photovoltaic performances of bulk-heterojunction organic solar cells. The fine tuning of the photophysical, morphological and processability properties with the aim of reaching higher and higher photocurrent efficiencies has prompted uninterrupted worldwide research on these peculiar families of organic compounds.

Keywords: photovoltaics ; Bulk-Heterojunction solar cells ; acceptor compounds ; fused-ring electron acceptors ; ITIC

1. Introduction

Photovoltaic cells are devices that are able to generate electrical power from solar energy. Although various technologies exist, including conventional silicon-based solar cells as well as emerging quantum dot and perovskite solar cells, organic solar cells (OSCs) with bulk heterojunction (BHJ) architecture offer unique advantages for specific applications. For example, OSC panels can be fabricated through low-cost ink-jet processes using environmentally friendly materials and can be scaled up for use in large-area devices. Because they are lightweight and flexible, they could be implemented in non-rigid architectures [1][2][3][4][5][6][7][8][9][10][11][12].

Conventional BHJ-OSCs are typically based on a blend of bicontinuous and interpenetrating electron donor (D) and electron acceptor (A) materials. The absorption of photons creates excitons that dissociate into charge carriers (holes and electrons) at the D/A interface, and the opposite polarity carrier materials transport holes and electrons through the donor and acceptor channels to the anode and cathode, respectively, where they are collected to be used as electrical power source. Efficient exciton dissociation in charge carriers and efficient transport to the electrodes need to be achieved to obtain appreciable power conversion efficiencies (PCEs). Materials need to be chosen to obtain an exergonic driving force for charge separation ($\Delta G_{CS} < 0$) and an efficient migration toward the electrodes.

Typical electron donor polymers exhibit a conjugated backbone on which pendant alkyl side chains, necessary for solubilization in organic solvents and processability, are present. OSCs based on fullerene electron acceptors (FAs) played a central role in the development of increasingly better performing devices, with a maximum PCE currently achieved at 11% [13]. FAs possess several advantages: photostability and efficient light harvesting, easy processability and high electron affinities [14]. 6,6-phenyl C_{61} butyric acid methyl ester ($PC_{61}BM$) and its C_{70}-based homologue ($PC_{71}BM$) are the most successful and widely used FAs for solution-processed BHJ OSCs. Their specific advantages can be summarized as follows: (i) strong tendency to accept electrons from common donor semiconductors; (ii) high electron mobility even in the composite form; (iii) ability to form favorable nanoscale morphological networks with donor materials; (iv) isotropy of charge transport; and (v) reversible electrochemical reduction [15]. Record efficiencies in OSCs have been the result of the development of new electron donor materials with improved properties, such as better spectral sensitivity, enhanced hole transport, and more favorable HOMO/LUMO (highest occupied molecular orbital/lowest unoccupied molecular orbital) energy levels, better matching with $PC_{61}BM$ or $PC_{71}BM$ HOMO/LUMO levels.

More recently, the focus in the development of OSCs has shifted to non-fullerene electron acceptors (NFAs) in combination with a polymeric electron donor in BHJ OSCs. In fact, the PCEs of such cells have increased dramatically since 2015, now reaching a high value of over 16% [16]. An ideal NFA should exhibit a) strong absorption coefficients in regions of the visible and NIR spectrum that are complementary to those in which the available electron donor polymers absorb; b) suitably matched energy levels for achieving exergonic charge separation with donors; c) the ability to form appropriate morphologies for charge separation and suitable percolation pathways for charge transport; and d) good molecular and morphological thermal and photostability. NFAs have a long history; indeed, the first reported bilayer OSCs used a perylene-based acceptor [17], and some early BHJ OSCs used electron-rich and electron-deficient poly(phenylenevinylene)s [18][19]. A wide variety of material classes have been examined as NFAs [20][21][22][23][24]. Many of the advances in NFA-containing OSCs are attributable to two classes of materials: rylene di-imides and fused-ring electron acceptors (FREAs) [25][26][27][28][29]. By far the best NFA-containing OSCs performances were achieved using

FREAs, well-defined organic compounds characterized by a push–pull architecture in which π-extended donating cores with four or more aromatic fused rings are flanked by two electron-withdrawing units (A–D–A molecular structures). Aromatic fused rings have been widely applied in the construction of high-mobility organic semiconductors because the extended conjugation in fused rings is beneficial to forming effective interchain π−π overlaps and enhancing intermolecular charge transport. Typical fused rings have high planarity and suffer from strong aggregation, leading to the formation of large crystalline domains. The introduction of rigid out-of-plane side chains onto the fused rings avoids the formation of large crystalline domains, and it optimizes the exciton diffusion/separation efficiencies. Meanwhile, the introduction of electron-withdrawing moieties (such as imide, amide, and cyano groups) end-capping the π-conjugated core can cause efficient mixing in forming the molecular orbitals, leading to stabilization of the molecular LUMO and reduction of the molecular HOMO–LUMO gap to red-shift absorbance.

Amongst FREAs, the IDIC/ITIC families of NFAs stood out in the last five years in terms of performances. The prototypical IDIC and ITIC molecules, namely, 2,2′-((2Z,2′Z)-((4,4,9,9-tetrahexyl-4,9-dihydro-s-indaceno[1,2-b:5,6-b′]dithiophene-2,7-diyl)bis(methanylylidene))bis(3-oxo-2,3-dihydro-1H-indene-2,1-diylidene))dimalononitrile (IDIC), and 3,9-bis(2-methylene-(3-(1,1-dicyanomethylene)-indanone)-5,5,11,11-tetrakis(4-hexylphenyl)-dithieno[2,3-d:2′,3′-d′]-s-indaceno[1,2-b:5,6-b′]dithiophene) (ITIC), a0 and b0, respectively, are shown in Figure 1. The molecular conjugated cores are decorated by spiro quaternary carbon stereocenters, bearing alkylaryl or alkyl substituents, which have been demonstrated to be essential for intermolecular separation and morphological optimization of the active layer [30][31]. The main differences between the IDIC and ITIC families are the presence of thiophene flanking units with a total of five fused planar aromatic units in the core for the former, and the presence of thienothiophene flanking units with a total of seven fused planar aromatic rings in the latter. We refer to flanking units to indicate a structured extension of the central core and to distinguish them from the endcap groups. Their synthesis is very similar and is comprised of cyclization to form and install the quaternary stereocenters on the preformed core and the final introduction of the electron-deficient end-capping moieties, usually indanedione derivatives, through a condensation reaction.

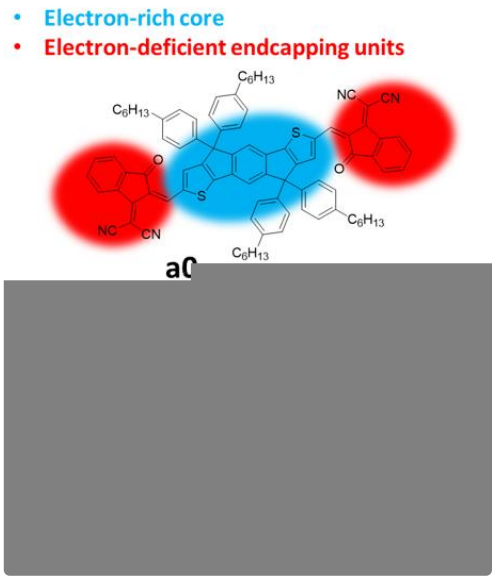

Figure 1. The prototypical member a0 and b0 of the IDIC and ITIC non-fullerene electron acceptors (NFA) families; the areas of possible modifications are highlighted.

With respect to other reviews on IDC/ITIC-type materials in the field of organic photovoltaics, we emphasize here the chemist's point of view, and we report a section on industrial considerations on their synthesis. The field is in continuous evolution, and other families of FREAs [32][33][34][35][36][37][38] have recently demonstrated extremely high potential.

2. Structural Modification of the IDIC/ITIC Core

The modification of the planar conjugated structure is one of the possible strategies to promote fine tuning of the optoelectronic and photovoltaic properties of the IDIC/ITIC families. Many recent reports have investigated the modification of this core by means of variations in the (a) central benzene ring, or (b) lateral thiophene or thienothienophene moieties. The most important modifications to the central core and lateral moieties are shown in Figures 2 and 3. The optical and electrochemical properties are summarized in Tables 1–4.

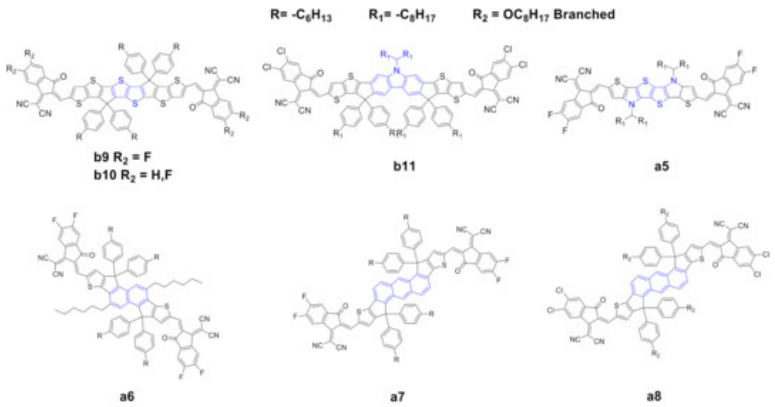

Figure 2. Structure of the acceptors of the IDIC/ITIC families, where the central core of a0 or b0 has been modified.

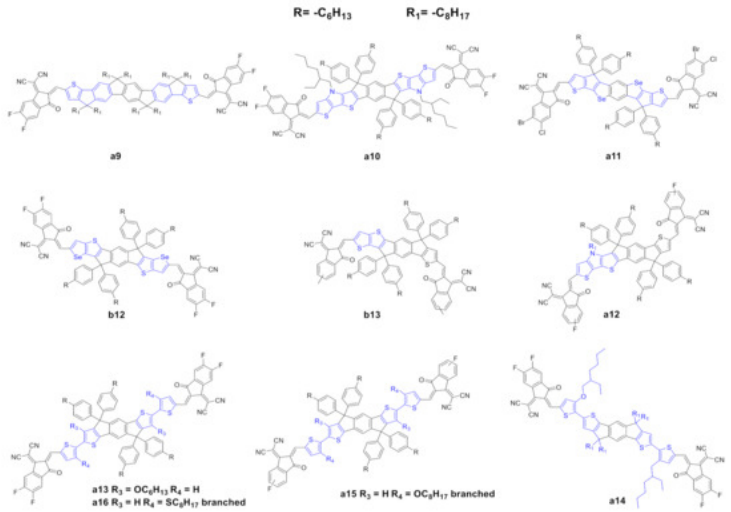

Figure 3. Structure of the of acceptors of the IDIC/ITIC families, where the flanking units of a0 or b0 have been modified.

Dai et al. [39] reported the synthesis of a novel thienothiophene (TT) core b9. The introduction of the TT moiety increases the electron density and extends the conjugation of the core compared to the classical benzene ring. The UV–vis spectra of b9 showed a remarkable red shift, with higher maximum extinction coefficient, a lower optical bandgap originated from a lower LUMO level and a higher electron mobility with respect to the prototypical ITIC b0. The authors also reported a simultaneously enhancement of V_{OC} and J_{sc} and, consequently, a higher PCE with respect to b0, other materials and equal parameters (Table 2). Li et al. [40] recently reported the synthesis of a novel NFA, b10, which essentially possesses the same structure as b9 but differs in terms of the end-capping groups: b10 possesses two fluorine atoms instead of four as in the case of b9. B10 has an absorption spectrum with a remarkable red shift due to the halogenated end-capping groups and a higher (almost double) maximum extinction coefficient with respect to ITIC b0; moreover, it has a higher HOMO and a lower LUMO which provoke a lower optical band gap. In terms of photovoltaic properties, b9 and b10 showed higher PCE compared with those of b0; the authors explained this as a consequence of complementary absorption with the donor, higher and more balanced charge mobility and a higher domain purity, which suppresses the bimolecular recombination and promotes charge transport, consequently increasing the PCE.

Chen *et al.* [41] reported the synthesis of a novel NFA b11 with a carbazole moiety instead of a benzene ring, combined with a chlorine-substituted end-capping group. The carbazole moiety has a strong electron-donating capacity, and, consequently, the resulting core is richer in terms of electron density. Such core substitution, however, gives rise in b11 to substantial red shift, higher HOMO and lower LUMO with respect to b0, and, in addition to the expected lower optical band gap, a higher extinction coefficient at the absorption maxima. In terms of photovoltaic properties, b11 showed higher V_{OC} and FF compared to those of b0, presumably as a consequence, as suggested by the authors, of higher electron/hole mobilities. The carbazole-based acceptor achieved the highest PCE for the binary BHJs reported to date in the literature with this class of NFAs (entry 13 in Table 2). Huang *et al.* [42] reported the synthesis of a novel NFA, a5, with a tetrathiophene central core in a structure with high planarity, resulting in an extended and electron-rich core compared with that of a0. The visible spectrum of a5 showed a remarkable red shift and a reduced HOMO/LUMO gap. In terms of photovoltaic properties (Table 1, entry 3), a5 showed much higher J_{sc} and FF with respect to a0, which the authors claim to be a result of higher electron mobility and a lower level of charge recombination. Zhu *et al.* [43] reported the synthesis of a novel NFA with a naphthalene core (a6); the optoelectronic properties are essentially the same as those of a0, apart from higher HOMO and LUMO levels, probably better matching the donor polymer, resulting in better performance in

terms of photovoltaic properties. An anthracene moiety was also proposed as a core by Yao et al. [44] and Feng et al. [45] (compounds a7 and a8). These scaffolds present an extension of the conjugation, resulting in a red-shifted UV–vis spectra and good extinction coefficients at λ_{max}. HOMO/LUMO energy differences, however, resulted to be higher for a7 and a8 than for a0. In terms of photovoltaic properties, however, a7 and a8 showed better performances when compared to those of a0, with higher values for all relevant parameters, namely, V_{OC}, J_{sc}, FF and PCE.

Table 1. Photovoltaic properties of best devices incorporating NFA acceptors shown in Figure 1.

Entry	Device	Voc (V) [i]	Jsc (mA·cm^{-2}) [j]	FF (%) [k]	PCE (%) [l]	Ref.
1	PDBT-T1:a0	0.89	14.61	63.0	8.19	[30]
2	J61: a1	1.15	10.84	66.17	8.25	[46]
3	PTB7-Th: a2	1.04	13.57	62.64	8.82	[47]
4	PBDB-T: a3	1.04	17.34	60.0	10.08	[48]
5	PBDB-T: a4	0.85	18.9	66.6	10.7	[49]
6	PTB7-TH: b0	0.81	14.21	59.1	6.80	[1]
7	PBDB-T-SF: b1	0.88	20.88	71.3	13.1	[29]
8	PBT1-C: b2	0.90	16.50	70.8	10.54	[50]
9	PBDB-T-2F: b3	0.79	22.67	75.2	13.45	[51]
10	PBDB-T: b4	0.93	18.11	71.52	12.07	[52]
11	J71: b5	0.92	18.41	74.2	12.5	[53]
12	PM6: b6	0.91	20.1	74.1	13.6	[54]
13	PBDB-T: b7	0.98	15.80	69.0	10.08	[55]
14	PBDB-T: b8	0.94	19.90	64.51	12.07	[56]

The modification of the central core and the corresponding fine tuning of the optoelectronic and photovoltaic properties represent the most important strategy to achieve highly performing IDIC/ITIC NFAs. Modification of the lateral moieties has also been addressed (Figure 4). Liu *et al.* [57] reported the synthesis of a novel NFA (a9) in which the two thiophene units of a0 were substituted with fluorene-type moieties. This substitution should affect the optoelectronic properties, and the UV spectra is slightly red-shifted with respect to a0 in solution, but such a red shift is not confirmed in thin films (Tables 3 and 4). Interestingly, a9 possesses a lower electron mobility, but higher photovoltaic parameters than those of a0; the authors explained this as a consequence of better complementary absorption with the donor, suppressed nonradioactive recombination loss, uniform and significantly decreased phase-separated morphology and a more efficiently suppressed charge recombination.

Sun et al. [58] reported the synthesis of a novel NFA, a10, in which the lateral thiophene moieties were substituted with dithienopyrrole moieties. The core extension in a10 allowed a remarkable red shift of the UV spectra to the NIR with a higher maximum molar absorption coefficient; moreover, the introduction of a much more electron rich-core led to a substantially higher HOMO, a lower optical band gap and a higher electron mobility compared with those of a0. In terms of photovoltaic properties, a10 showed better photovoltaic parameters than a0. Wan *et al.* [59] and Lin *et al.* [60] reported the synthesis of two novel NFAs, a11 and b12. These acceptors, despite the different halides in the end-capping groups, have a regioisomeric scaffold. A11 and b12 present a remarkable and slightly red-shift UV spectra compared with a0 and b0, respectively, induced by the introduction of the selenium heterocycle. In terms of photovoltaic properties, interestingly, a11 showed higher PCE than b12.

Table 2. Optical and electrochemical properties of acceptors a5–a8 and b9–b11.

Entry	Compound	T_d (°C)[a]	(nm)[b]	(nm)[c]	(eV)[d]	e ($_{max}$) (M^{-1}·L^{-1})[e]	HOMO (eV)	LUMO (eV)	m^{SCLC} (cm^2·V^{-1}·s^{-1})[f]	Ref.
1	a0		664	716	1.62	2.4×10^5	−5.69	−3.91	1.1×10^{-3}	[30]

2	a5				1.32		−5.52	−4.11	3.94×10^{-4}	[42]
3	a6	384	696	730	1.55	1.8×10^{5}	−5.41	−3.78	1×10^{-3}	[43]
4	a7		718	778	1.68		−5.69	−4.01		[61]
5	a8		691	709	1.60	2.2×10^{5}	−5.71	−3.89		[45]
6	b0	345	664	702	1.59	1.3×10^{5}	−5.48	−3.83	3.0×10^{-4}	[1]
7	b9	331	788	862	1.27	2.3×10^{5}	–5.43	–4.00	1.5×10^{-3}	[39]
8	b10	328	782	836	1.32	2.0×10^{5}	–5.36	–3.92	1.2×10^{-3}	[40]
9	b11	338	690	753	1.47	2.3×10^{5}	−5.72	−4.03		[41]

(a) Decomposition temperature; (b) λ_{max} in solution; (c) λ_{max} in thin films; (d) optical band gap; (e) extinction coefficient at λ_{max}; (f) electron mobility.

Table 3. Photovoltaic properties of the best devices incorporating NFA acceptors shown in Figure 3.

Entry	Device	V_{oc} (V)[i]	J_{sc} (mA·cm^{-2})[j]	FF (%)[k]	PCE (%)[l]	Ref.
1	PDBT-T1: a0	0.89	14.6	63.0	8.2	[30]
2	PBDB-T: a5	0.78	23.2	73.0	13.2	[42]
3	FTAZ: a6	0.90	19.7	69.3	12.3	[43]
4	PBDB-TF: a7	0.93	19.0	73.9	13.1	[61]
5	PBDB-TF: a8	0.90	19.5	75.5	13.3	[45]
6	PTB7-TH: b0	0.81	14.2	59.1	6.8	[1]
7	PTB7-Th: b9	0.64	25.1	67.6	10.9	[39]
8	PTB7-Th: b10	0.74	24.0	67.1	12.0	[40]
9	PM6: b11	0.92	22.6	74.0	15.4	[41]

(i) Open circuit voltage, (j) short-circuit current density, (k) fill factor, (l) power conversion efficiency.

Table 4. Optical and electrochemical properties of acceptors a9–a12 and b12–b13.

Entry	Compound	T_d (°C)[a]	(nm)[b]	(nm)[c]	(eV)[d]	e (λ_{max}) (M^{-1}·L^{-1})[e]	HOMO (eV)	LUMO (eV)	m^{SCLC} (cm^2·V^{-1}·s^{-1})[f]	Ref.

1	a0		664	716	1.62	2.4×10^5	−5.69	−3.91	1.1×10^{-3}	[30]
2	a9		678	704	1.61		−5.71	−3.96	3.53×10^{-4}	[57]
3	a10	377	769	821	1.39	3.51×10^5	−5.42	−3.95		[58]
4	a11	350	736	793	1.39		−5.64	−3.95		[59]
5	a12	350	739	775	1.44		−5.51	−3.96		[62]
6	a13		723	765	1.44	9.9×10^4	−5.54	−3.94		[63]
7	a14		790	850	1.28	1.32×10^5	−5.44	−4.15		[64]
8	a15	345	794	839	1.31		−5.34	−4.06		[65]
9	a16	334	751	831	1.30		−5.54	−4.05	2.65×10^{-4}	[66]
10	b0	345	664	702	1.59	1.3×10^5	−5.48	−3.83	3.0×10^{-4}	[1]
11	b12		698	752	1.44	2.14×10^5	−5.52	−3.90		[60]
12	b13	300	664	696	1.65	2.00×10^5	−5.60	–3.87	9.64×10^{-4}	[67]

(a) Decomposition temperature; (b) λ_{max} in solution; (c) λ_{max} in thin films; (d) optical band gap; (e) extinction coefficient at λ_{max}; (f) electron mobility.

Table 5. Photovoltaic properties of the best devices incorporating NFA acceptors shown in Figure 4.

Entry	Device	Voc (V)[i]	Jsc (mA·cm^{-2})[j]	FF (%)[k]	PCE (%)[l]	Ref.
1	PDBT-T1: a0	0.89	14.61	63.0	8.19	[30]
2	PBDB-T2F: a9	0.980	17.60	76.0	13.1	[57]
3	PBDB-T: a10	0.852	21.9	69.8	13.1	[58]
4	PM7: a11	0.830	22.91	76.5	14.54	[59]
5	PBDB-T: a12	0.860	22.4	72.4	14.0	[62]
7	PBDB-T: a13	0.850	20.87	72.0	12.79	[63]
8	PTB7-Th: a14	0.74	26.30	67.0	13.1	[64]
9	PTB7-Th: a15	0.817	21.90	65.0	12.1	[65]

10	PTB7-Th: a16	0.750	25.3	69.3	13.2	[66]
11	PTB7-TH: b0	0.81	14.21	59.1	6.80	[1]
12	PBDB-T-2F: b12	0.846	20.21	75.2	13.05	[60]
13	PBDB-T: b13	0.910	16.02	76.8	11.2	[67]

(i) Open circuit voltage, (j) short-circuit current density, (k) fill factor, (l) power conversion efficiency.

Asymmetric scaffolds represent an interesting strategy to promote fine tuning of the optoelectronic properties and a way to achieve high-performance OSCs. Gao *et al.* [67] reported the synthesis of a novel NFA, b13, with an asymmetrical scaffold; it can be categorized as an ITIC with a thiophene instead of a thienothiophene. B13 showed basically the same UV spectra with a slightly higher molar extinction coefficient; moreover, b13 has a higher HOMO and a comparable LUMO with respect to b0. Interestingly, the authors observed that the asymmetric scaffold of b13 possessed a higher dipole moment, leading to a high polarity molecule, which could be useful in order to increase the solubility of these molecules in a much more polar solvent than the conventional ones used in device fabrication. In terms of photovoltaic properties, b13 showed higher values for all parameters vs. b0, and consequently higher PCE. The authors explained these results as a consequence of higher and more balanced carrier mobilities, better dissociation probability and charge collection ability, minor bimolecular recombination and excellent morphology. Last year, Yang *et al.* [62] reported the synthesis of a novel asymmetric NFA, a12, which possesses a dithienopyrrole moiety. A12 showed a remarkable red shift compared to a0, and, in terms of photovoltaic properties, it showed higher values for all parameters vs. a0, and consequently higher PCE.

NFA molecules must be soluble in common organic solvents in order to be processable. Alkyl side chains ensure good solubility in these solvents; the introduction of alkyl chains is, however, associated with other problems such as impeding the ordered packing of molecules, which decreases the charge transport ability, lowers carrier mobility, and deteriorates device performance. Liu et al. [63] synthetized a novel NFA, a13, which bears two hexyloxy groups at its central core in order to modulate the photophysical, photovoltaic and morphological properties. The side chain introduction and the two terminal thiophene rings of a13 provoke a remarkable red shift with respect to a0. In terms of photovoltaic properties, a13 shows higher values for all parameters vs. a0, and, consequently, higher PCE. It is worth noting that the photovoltaic performances were achieved with spin-coated active layers—as stated by the authors, no extra treatment, such as using additives or annealing, was needed. Lee *et al.* [64] synthetized a novel NFA, a14, which possesses an asymmetrical side chain substitution pattern. A14 showed a remarkable red shifted UV–vis spectrum when compared to a0, while, in terms of HOMO/LUMO levels, a14 showed a lower optical band gap. In terms of photovoltaic properties, it showed higher values for all parameters vs. a0, and consequently higher PCE as a primary consequence of favorable BHJ morphology for efficient charge separation and transport. Lee *et al.* [65] and Chen et al. [66] expended this work by synthetizing two novel NFAs, a15 and a16, which contain the same side chains but different heteroatoms onto the flanking thiophene rings. Both acceptors showed remarkable red-shifted UV–vis spectra when compared to those of a0. The optical bandgaps are essentially the same for both acceptors. In terms of photovoltaic properties, they showed higher values for all parameters vs. a0, and consequently higher PCE. The authors claim an efficient wavelength collection near NIR, favorable BHJ morphology, well-ordered molecular orientation, and tight face-on packing.

References

1. Lin, Y.; Wang, J.; Zhang, Z.-G.; Bai, H.; Li, Y.; Zhu, D.; Zhan, X. An Electron Acceptor Challenging Fullerenes for Efficient Polymer Solar Cells. Mater. 2015, 27, 1170–1174.
2. Xu, Y.-X.; Chueh, C.-C.; Yip, H.-L.; Ding, F.-Z.; Li, Y.-X.; Li, C.-Z.; Li, X.; Chen, W.-C.; Jen, A.K.-Y. Improved Charge Transport and Absorption Coefficient in Indacenodithieno[3,2-b]thiophene-based Ladder-Type Polymer Leading to Highly Efficient Polymer Solar Cells. Mater. 2012, 24, 6356–6361.
3. Intemann, J.J.; Yao, K.; Li, Y.-X.; Yip, H.-L.; Xu, Y.-X.; Liang, P.-W.; Chueh, C.-C.; Ding, F.-Z.; Yang, X.; Li, X.; et al. Highly Efficient Inverted Organic Solar Cells Through Material and Interfacial Engineering of Indacenodithieno[3,2-b]thiophene-Based Polymers and Devices. Funct. Mater. 2014, 24, 1465–1473.
4. Li, Y.; Yao, K.; Yip, H.-L.; Ding, F.-Z.; Xu, Y.-X.; Li, X.; Chen, Y.; Jen, A.K.-Y. Eleven-Membered Fused-Ring Low Band-Gap Polymer with Enhanced Charge Carrier Mobility and Photovoltaic Performance. Funct. Mater. 2014, 24, 3631–

3638.

5. Wang, G.; Melkonyan, S.F.; Facchetti, A.; Marks, T.J. All-Polymer Solar Cells: Recent Progress, Challenges, and Prospects. Chem. Int. Ed. 2019, 58, 4129–4142.
6. Chen, L.X. Organic Solar Cells: Recent Progress and Challenges. ACS Energy Lett. 2019, 4, 2537–2539.
7. Yin, H.; Yan, C.; Hu, H.; Ho, J.K.; Zhan, X.; So, G.L.S.K. Recent progress of all-polymer solar cells–From chemical structure and device physics to photovoltaic performance. Sci. Eng. R Rep. 2020, 140, 1005422.
8. Karunakaran, S.K.; Arumugam, G.M.; Yang, W.; Ge, S.; Khan, S.N.; Li, X.; Yang, G. Recent progress in inkjet-printed solar cells. Mater. Chem. A 2019, 7, 13873–13902.
9. Qin, J.; Lan, L.; Chen, S.; Huang, F.; Shi, H.; Chen, W.; Xia, H.; Sun, K.; Yang, C. Recent Progress in Flexible and Stretchable Organic Solar Cells. Funct. Mater. 2020, 30, 2002529.
10. Ryu, H.S.; Park, S.Y.; Lee, H.T.; Kim, J.Y.; Woo, H.Y. Recent progress in indoor organic photovoltaics. Nanoscale 2020, 12, 5792–5804.
11. Nitti, A.; Signorile, M.; Boiocchi, M.; Bianchi, G.; Po, R.; Pasini, D. Conjugated Thiophene-Fused Isatin Dyes through Intramolecular Direct Arylation. Org. Chem. 2016, 81, 11035–11042.
12. Nitti, A.; Bianchi, G.; Po, R.; Swager, T.M.; Pasini, D. Domino Direct Arylation and Cross-Aldol for Rapid Construction of Extended Polycyclic π-Scaffolds. Am. Chem. Soc. 2017, 139, 8788–8791.
13. Chochos, C.L.; Katsouras, A.; Gasparini, N.; Koulogiannis, C.; Ameri, T.; Brabec, C.J.; Avgeropoulos, A. Rational Design of High-Performance Wide-Bandgap (≈2 eV) Polymer Semiconductors as Electron Donors in Organic Photovoltaics Exhibiting High Open Circuit Voltages (≈1 V). Rapid Commun. 2017, 38, 1600614.
14. Gasparini, N.; Katsouras, A.; Prodromidis, M.I.; Avgeropoulos, A.; Baran, D.; Salvador, M.; Fladischer, S.; Spiecker, E.; Chochos, C.L.; Ameri, T.; et al. Photophysics of Molecular-Weight-Induced Losses in Indacenodithienothiophene-Based Solar Cells. Funct. Mater. 2015, 25, 4898–4907.
15. Cai, Y.; Zhang, X.; Xue, X.; Wei, D.; Huo, L.; Sun, Y. High-Performance Wide-Bandgap Copolymers Based on Indacenodithiophene and Indacenodithieno[3,2-b]thiophene Units. Mater. Chem. C 2017, 5, 7777–7783.
16. Sun, H.; Liu, T.; Yu, J.; Lau, T.-K.; Zhang, G.; Zhang, Y.; Su, M.; Tang, Y.; Ma, R.; Liu, B.; et al. A monothiophene unit incorporating both fluoro and ester substitution enabling high-performance donor polymers for non-fullerene solar cells with 16.4% efficiency. Energy Environ. Sci. 2019, 12, 3328–3337.
17. Vandewal, K.; Tvingstedt, K.; Gadisa, A.; Inganäs, O.; Manca, J.V. Relating the open-circuit voltage to interface molecular properties of donor: Acceptor bulk heterojunction solar cells. Rev. B 2010, 81, 125204.
18. Hou, J.; Inganäs, O.; Friend, R.H.; Gao, F. Organic solar cells based on non-fullerene acceptors. Mater. 2018, 17, 119–128.
19. Eastham, N.D.; Logsdon, J.L.; Manley, E.F.; Aldrich, T.J.; Leonardi, M.J.; Wang, G.; Powers-Riggs, N.E.; Young, R.M.; Chen, L.X.; Wasielewski, M.R.; et al. Hole-Transfer Dependence on Blend Morphology and Energy Level Alignment in Polymer: ITIC Photovoltaic Adv. Mater. 2018, 30, 1704263.
20. Srivani, D.; Agarwal, A.; Bhosale, S.V.; Puvad, A.L.; Xiang, W.; Evans, R.A.; Gupta, A.; Bhosale, S.V. Naphthalene diimide-based non-fullerene acceptors flanked by open-ended and aromatizable acceptor functionalities. Commun. 2017, 53, 11157–11160.
21. Sung, M.J.; Huang, M.; Moon, S.H.; Lee, T.H.; Park, S.Y.; Kim, J.Y.; Kwon, S.K.; Choi, H.; Kim, Y.H. Naphthalene diimide-based small molecule acceptors for fullerene-free organic solar cells. Energy 2017, 150, 90–95.
22. Jina, R.; Wang, F.; Guana, R.; Zhenga, X.; Zhang, T. Design of perylene-diimides-based small-molecules semiconductors for organic solar cells. Phys. 2017, 115, 1591–1597.
23. Jo, J.W.; Jung, J.W.; Wang, H.-W.; Kim, P.; Russell, T.P.; Jo, W.H. Fluorination of Polythiophene Derivatives for High Performance Organic Photovoltaics. Mater. 2015, 27, 4865−4870.
24. Jung, W.J.; Jo, W.H. Low-Bandgap Small Molecules as Non-Fullerene Electron Acceptors Composed of Benzothiadiazole and Diketopyrrolopyrrole for All Organic Solar Cells. Mater. 2015, 27, 6038−6043.
25. Zhao, F.; Dai, S.; Wu, Y.; Zhang, Q.; Wang, J.; Jiang, L.; Ling, Q.; Wei, Z.; Ma, W.; You, W.; et al. Single-Junction Binary-Blend Nonfullerene Polymer Solar Cells with 12.1% Efficiency. Mater. 2017, 29, 1700144.
26. Cui, Y.; Yao, H.; Gao, B.; Qin, Y.; Zhang, S.; Yang, B.; He, C.; Xu, B.; Hou, J. Fine-Tuned Photoactive and Interconnection Layers for Achieving over 13% Efficiency in a Fullerene-Free Tandem Organic Solar Cell. Am. Chem. Soc. 2017, 139, 7302−7309.

27. Xie, D.; Liu, T.; Gao, W.; Zhong, C.; Huo, L.; Luo, Z.; Wu, K.; Xiong, W.; Liu, F.; Sun, Y.; et al. A Novel Thiophene-Fused Ending Group Enabling an Excellent Small Molecule Acceptor for High-Performance Fullerene-Free Polymer Solar Cells with 11.8% Efficiency. Solar RRL 2017, 1, 1700044.

28. Wang, J.; Wang, W.; Wang, X.; Wu, Y.; Zhang, Q.; Yan, C.; Ma, W.; You, W.; Zhan, X. Enhancing Performance of Nonfullerene Acceptors via Side-Chain Conjugation Strategy. Mater. 2017, 29, 1702125.

29. Zhao, W.; Li, S.; Yao, H.; Zhang, S.; Zhang, Y.; Yang, B.; Hou, J. Molecular Optimization Enables over 13% Efficiency in Organic Solar Cells. Am. Chem. Soc. 2017, 139, 7148−7151.

30. Lin, Y.; He, Q.; Zhao, F.; Huo, L.; Mai, J.; Lu, X.; Su, C.-J.; Li, T.; Wang, J.; Zhu, J.; et al. A Facile Planar Fused-Ring Electron Acceptor for As-Cast Polymer Solar Cells with 8.71% Efficiency. Am. Chem. Soc. 2016, 138, 2973−2976.

31. Yuan, J.; Zhang, Y.; Zhou, L.; Zhang, G.; Yip, H.-L.; Lau, T.-K.; Lu, X.; Zhu, C.; Peng, H.; Johnson, P.A.; et al. Single-Junction Organic Solar Cell with over 15% Efficiency Using Fused-Ring Acceptor with Electron-Deficient Core. Joule 2019, 3, 1140–1151.

32. Fei, Z.; Eisner, F.D.; Jiao, X.; Azzouzi, M.; Röhr, J.A.; Han, Y.; Shahid, M.; Chesman, A.S.R.; Easton, C.D.; McNeill, C.R.; et al. An Alkylated Indacenodithieno[3,2-b]thiophene-Based Nonfullerene Acceptor with High Crystallinity Exhibiting Single Junction Solar Cell Efficiencies Greater than 13% with Low Voltage Losses. Mater. 2018, 30, 1705209.

33. Zhang, Z.; Guang, S.; Yu, J.; Wang, H.; Cao, J.; Du, F.; Wang, X.; Tang, W. Over 15.5% efficiency organic solar cells with triple side chain engineered ITIC. Bull. 2020, 65, 1533–1536.

34. Yang, C.; Zhang, S.; Ren, J.; Gao, M.; Bi, P.; Ye, L.; Hou, J. Molecular design of a non-fullerene acceptor enables a P3HT-based organic solar cell with 9.46% efficiency. Energy Environ. Sci. 2020, 13, 2864–1536.

35. Asakawa, M.; Brown, C.L.; Pasini, D.; Stoddart, J.F.; Wyatt, P.G. Enantioselective Recognition of Amino Acids by Axially-Chiral □-Electron Deficient Receptors. Org. Chem. 1996, 61, 7234–7235.

36. Park, S.H.; Park, S.; Lee, S.; Kim, J.; Ahn, H.; Kim, B.J.; Chae, B.; Son, H.J. Developement of highly efficient large area organic photovoltaic module: Effects of nonfullerene acceptor. Nano Energy 2020, 77, 105147.

37. Meredith, P.; Li, W.; Armin, A. Nonfullerene Acceptors: A Renaissance in Organic Photovoltaics? Energy Mater. 2020, 10, 2001788.

38. Fox, D.; Metrangolo, P.; Pasini, D.; Pilati, T.; Resnati, G.; Terraneo, G. Site Selective Supramolecular Synthesis of Halogen Bonded Cocrystals Incorporating the Photoactive Azo Group. CrystEngComm 2008, 10, 1132–1136.

39. Dai, S.; Li, T.; Wang, W.; Xiao, Y.; Lau, T.K.; Li, Z.; Liu, K.; Lu, X.; Zhan, X. Enhancing the Performance of Polymer Solar Cells via Core Engineering of NIR-Absorbing Electron Acceptors. Adv. Mater. 2018, 30, 1706571.

40. Li, T.; Dai, S.; Ke, Z.; Yang, L.; Wang, J.; Yan, C.; Ma, W.; Zhan, X. Fused Tris(thienothiophene)-Based Electron Acceptor with Strong Near-Infrared Absorption for High-Performance As-Cast Solar Cells. Adv. Mater. 2018, 30, 1705969.

41. Chen, T.-W.; Peng, K.-L.; Li, Y.-W.; Su, Y.-J.; Ma, K.-J.; Hong, L.; Chang, C.-C.; Hou, J.; Hsu, C.-S. A chlorinated nonacyclic carbazole-based acceptor affords over 15% efficiency in organic solar cells. J. Mater. Chem. A 2020, 8, 1131–1137.

42. Huang, C.; Liao, X.; Gao, K.; Zuo, L.; Lin, F.; Shi, X.; Li, C.-Z.; Liu, H.; Li, X.; Liu, F.; et al. Highly Efficient Organic Solar Cells Based on S,N-Heteroacene NonFullerene Acceptors. Chem. Mater. 2018, 30, 5429–5434.

43. Zhu, J.; Ke, Z.; Zhang, Q.; Wang, J.; Dai, S.; Wu, Y.; Xu, Y.; Lin, Y.; Ma, W.; You, W.; et al. Naphthodithiophene-Based Nonfullerene Acceptor for High-Performance Organic Photovoltaics: Effect of Extended Conjugation. Adv. Mater. 2018, 30, 1704713.

44. Yao, C.; Liu, B.; Zhu, Y.; Hong, L.; Miao, J.; Hou, J.; He, F.; Meng, H. Highly fluorescent anthracene derivative as a non-fullerene acceptor in OSCs with small non-radiative energy loss of 0.22 eV and high PCEs of over 13%. J. Mater. Chem. A 2019, 7, 10212–10216.

45. Feng, H.; Yi, Y.-Q.-Q.; Ke, X.; Yan, J.; Zhang, Y.; Wan, X.; Li, C.; Zheng, N.; Xie, Z.; Chen, Y. New Anthracene-Fused Nonfullerene Acceptors for High-Efficiency Organic Solar Cells: Energy Level Modulations Enabling Match of Donor and Acceptor. Adv. Energy Mater. 2019, 9, 1803541.

46. Tang, A.; Xiao, B.; Wang, Y.; Gao, F.; Tajima, K.; Bin, H.; Zhang, Z.-G.; Li, Y.; Wei, Z.; Zhou, E. Simultaneously Achieved High Open-Circuit Voltage and Efficient Charge Generation by Fine-Tuning Charge-Transfer Driving Force in Nonfullerene Polymer Solar Cells. Adv. Funct. Mater. 2018, 28, 1704507.

47. Tang, L.-M.; Xiaob, J.; Baia, W.-Y.; Lia, Q.-Y.; Wanga, H.-C.; Miaoc, M.-S.; Yipb, H.-L.; Xua, Y.-X. End-chain effects of non-fullerene acceptors on polymer solar cells. Org. Electron 2019, 64, 1–6.

48. Kolhe, N.B.; West, S.M.; Tran, D.K.; Ding, X.; Kuzuhara, D.; Yoshimoto, N.; Koganezawa, T.; Jenekhe, S.A. Designing High Performance Nonfullerene Electron Acceptors with Rylene Imides for Efficient Organic Photovoltaics. Chem. Mater. 2020, 32, 195–204.

49. Qu, J.; Zhao, Q.; Zhou, J.; Lai, H.; Liu, T.; Li, D.; Chen, W.; Xie, Z.; He, F. Multiple Fused Ring-Based Near-Infrared Nonfullerene Acceptors with an Interpenetrated Charge-Transfer Network. Chem. Mater. 2019, 31, 1664–1671.

50. Li, X.; Li, C.; Ye, L.; Weng, K.; Fu, H.; Ryu, H.S.; Wei, D.; Sun, X.; Woo, H.Y.; Sun, Y. Asymmetric A–D–p–A-type nonfullerene small molecule acceptors for efficient organic solar cells. J. Mater. Chem. A 2019, 7, 19348–19354.

51. Zhang, H.; Yao, H.; Hou, J.; Zhu, J.; Zhang, J.; Li, W.; Yu, R.; Gao, B.; Zhang, S.; Hou, J. Over 14% Efficiency in Organic Solar Cells Enabled by Chlorinated Nonfullerene Small-Molecule Acceptors. Adv. Mater. 2018, 30, 1800613.

52. Li, M.; Zhou, Y.; Zhang, J.; Song, J.; Bo, Z. Tuning the dipole moments of nonfullerene acceptors with an asymmetric terminal strategy for highly efficient organic solar cells. J. Mater. Chem. A 2019, 7, 8889–8896.

53. Luo, Z.; Bin, H.; Liu, T.; Zhang, Z.-G.; Yang, Y.; Zhong, C.; Qiu, B.; Li, G.; Gao, W.; Xie, D.; et al. Fine-Tuning of Molecular Packing and Energy Level through Methyl Substitution Enabling Excellent Small Molecule Acceptors for Nonfullerene Polymer Solar Cells with Efficiency up to 12.54%. Adv. Mater. 2018, 30, 1706124.

54. Luo, Z.; Liu, T.; Wang, Y.; Zhang, G.; Sun, R.; Chen, Z.; Zhong, C.; Wu, J.; Chen, Y.; Zhang, M.; et al. Reduced Energy Loss Enabled by a Chlorinated Thiophene-Fused Ending-Group Small Molecular Acceptor for Efficient Nonfullerene Organic Solar Cells with 13.6% Efficiency. Adv. Energy Mater. 2019, 9, 1900041.

55. Firdaus, Y.; He, Q.; Lin, Y.; Nugroho, F.A.A.; Le Corre, V.M.; Yengel, E.; Balawi, A.H.; Seitkhan, A.; Laquai, F.; Langhammer, C.; et al. Novel wide-bandgap non-fullerene acceptors for efficient tandem organic solar cells. J. Mater. Chem. A 2020, 8, 1164–1175.

56. Chang, S.-L.; Hung, K.-E.; Cao, F.-Y.; Huang, K.-H.; Hsu, C.-S.; Liao, C.-Y.; Lee, C.-H.; Cheng, Y.-J. Isomerically Pure Benzothiophene-Incorporated Acceptor: Achieving Improved Voc and Jsc of Nonfullerene Organic Solar Cells via End Group Manipulation. ACS Appl. Mater. Interfaces 2019, 11, 33179–33187.

57. Liu, G.; Jia, J.; Zhang, K.; Jia, X.; Yin, Q.; Zhong, W.; Li, L.; Huang, F.; Cao, Y. 15% Efficiency Tandem Organic Solar Cell Based on a Novel Highly Efficient Wide-Bandgap Nonfullerene Acceptor with Low Energy Loss. Adv. Energy Mater. 2019, 9, 1803657.

58. Sun, J.; Ma, X.; Zhang, Z.; Yu, J.; Zhou, J.; Yin, X.; Yang, L.; Geng, R.; Zhu, R.; Zhang, F.; et al. Side chain engineering on Dithieno[3,2-b:2′,3′-d]pyrrol Fused Nonfullerene Acceptors Enabling Over 13% Efficiency for Organic Solar Cells. Mater. Chem. Front. 2019, 3, 702–708.

59. Wan, S.-S.; Xu, X.; Jiang, Z.; Yuan, J.; Mahmood, A.; Yuan, G.-Z.; Liu, K.-K.; Ma, W.; Peng, Q.; Wang, J.-L. A bromine and chlorine concurrently functionalized end group for benzo[1,2-b:4,5-b′]diselenophene-based non-fluorinated acceptors: A new hybrid strategy to balance the crystallinity and miscibility of blend films for enabling highly efficient polymer solar cells. J. Mater. Chem. A 2020, 8, 4856–4867.

60. Lin, F.; Zuo, L.; Gao, K.; Zhang, M.; Jo, S.B.; Liu, F.; Jen, A.K.-Y. Regio-Specific Selenium Substitution in Non-Fullerene Acceptors for Efficient Organic Solar Cells. Chem. Mater. 2019, 31, 6770–6778.

61. Yao, C.; Liu, B.; Zhu, Y.; Hong, L.; Miao, J.; Hou, J.; He, F.; Meng, H. Highly fluorescent anthracene derivative as a non-fullerene acceptor in OSCs with small non-radiative energy loss of 0.22 eV and high PCEs of over 13%. J. Mater. Chem. A 2019, 7, 10212–10216.

62. Yang, L.; Song, X.; Yu, J.; Wang, H.; Zhang, Z.; Geng, R.; Cao, J.; Baran, D.; Tang, W. Tuning of the conformation of asymmetric nonfullerene acceptors for efficient organic solar cells. J. Mater. Chem. A 2019, 7, 22279–22286.

63. Liu, Y.; Li, M.; Zhou, X.; Jia, Q.-Q.; Feng, S.; Jiang, P.; Xu, X.; Ma, W.; Li, H.-B.; Bo, Z. Nonfullerene Acceptors with Enhanced Solubility and Ordered Packing for HighEfficiency Polymer Solar Cells. ACS Energy Lett. 2018, 3, 1832–1839.

64. Lee, J.; Song, S.; Huang, J.; Du, Z.; Lee, H.; Zhu, Z.; Ko, S.-J.; Nguyen, T.-Q.; Kim, J.Y.; Cho, K.; et al. Bandgap Tailored Nonfullerene Acceptors for Low-Energy-Loss Near-Infrared Organic Photovoltaics. ACS Mater. Lett. 2020, 2, 395–402.

65. Lee, J.; Ko, S.-J.; Seifrid, M.; Lee, H.; McDowell, C.; Luginbuhl, B.R.; Karki, A.; Cho, K.; Nguyen, T.-Q.; Bazan, G.C. Design of Nonfullerene Acceptors with Near-Infrared Light Absorption Capabilities. Adv. Energy Mater. 2018, 8, 1801209.

66. Chen, J.; Li, G.; Zhu, Q.; Guo, X.; Fan, Q.; Ma, W.; Zhang, M. Highly efficient near-infrared and semitransparent polymer solar cells based on an ultra-narrow bandgap nonfullerene acceptor. J. Mater. Chem. A 2019, 7, 3745–3751.

67. Gao, W.; Zhang, M.; Liu, T.; Ming, R.; An, Q.; Wu, K.; Xie, D.; Luo, Z.; Zhong, C.; Liu, F.; et al. Asymmetrical Ladder-Type Donor-Induced Polar Small Molecule Acceptor to Promote Fill Factors Approaching 77% for High-Performance

Nonfullerene Polymer Solar Cells. Adv. Mater. 2018, 30, 1800052.